Electrochemical response in ionic polymer transducers: An experimental and theoretical study

Thomas Wallmersperger, Barbar J. Akle, Donald J. Leo, Bernd Kröplin

Electrochemical response in ionic polymer transducers: An experimental and theoretical study

Thomas Wallmersperger, Barbar J. Akle, Donald J. Leo, Bernd Kröplin

PII: S0266-3538(07)00245-X
DOI: 10.1016/j.compscitech.2007.06.001
Reference: CSTE 3736

To appear in: *Composites Science and Technology*

Received Date: 5 April 2007
Revised Date: 4 June 2007
Accepted Date: 4 June 2007

Please cite this article as: Wallmersperger, T., Akle, B.J., Leo, D.J., Kröplin, B., Electrochemical response in ionic polymer transducers: An experimental and theoretical study, *Composites Science and Technology* (2007), doi: 10.1016/j.compscitech.2007.06.001

Electrochemical response in ionic polymer transducers: An experimental and theoretical study

Thomas Wallmersperger [a,b,*], Barbar J. Akle [b], Donald J. Leo [b], Bernd Kröplin [a]

[a] *Institute for Statics and Dynamics of Aerospace Structures*
University of Stuttgart, Stuttgart, Germany

[b] *Center for Intelligent Material Systems and Structures*
Virginia Polytechnic Institute and State University, Blacksburg, VA

Abstract

Ionomeric polymer transducers consist of an ion-conducting membrane, usually Nafion or Flemion, sandwiched between two metal electrodes. By applying a low voltage (up to 2 V), a relatively large bending deformation (> 5% strain) can be obtained. In this work, a chemo-electrical model based on the Nernst-Planck equations for charge conduction is experimentally calibrated. The applied model can realize a variable behavior of the current and charge density in space and time by varying the dielectric permittivity and the diffusion constant. It is shown that an increase of the permittivity results in slower time decay at constant peak current density for an applied electric potential step. The charge density accumulated at the electrode also increases with the dielectric permittivity. An increase of the diffusion coefficient increases the peak current and results in a smaller time decay constant. Experimental investigations are conducted for a proton based Nafion 117 sample

sandwiched between gold, silver, and copper flat electrodes. A comparison between the measured data and the predicted response for flat electrodes shows a good agreement for both, peak current density and charge density.

Key words: A. Polymer-matrix composites (PMCs); A. Smart materials; B. Modelling; B. Electrical properties; C. Finite element analysis (FEA)

1 INTRODUCTION

Ionomeric polymer transducers (IPT) also known as ionic polymer metal composites (IPMC) belong to the class of electroactive polymer actuators. It has been shown that they can produce actuation strains in the order of 5% to 10% [1] upon the application of a 2V electric potential [2,3]. Recent developments by our group have demonstrated that ionomeric polymer transducers can be fabricated using a novel "Direct Assembly Process". Using ionic liquids as diluents in IPTs enables superior operation in air [4]. Furthermore, ionic polymer transducers are reliable for over 1 million cycles.

As shown in Fig. 1, an ionomeric polymer transducer that consists of a solid electrolyte, usually Nafion or Flemion, sandwiched between two conductive electrodes [5] will bend upon the application of an electric field. If the actuator is not restrained it will produce a large curvature which can be modulated by changing the applied potential. Restraining the actuator to have zero motion will produce a blocked force that is related to the geometry of the actuator, the material properties, and the applied potential.

* Corresponding autor: Phone: +49/711/685-69542; Fax: +49/711/685-63706
Email address: wallmers@isd.uni-stuttgart.de (Thomas Wallmersperger).

Recently it has been shown in both, experiment and theory, that the electrode layer is a critical component that strongly influences the transducer performance. Experimental work by Akle et al. [6] has correlated the actuation properties of the transducer with the capacitance of the transducer. This result was consistent for ionomers with substantial differences in composition; this strongly suggests that charge accumulation at the polymer-metal interface is a determining factor in the strain and strain rate generated during actuation. This experimental result is supported by physics-based modeling efforts [7,8,9] which emphasize the role played by the boundary layer forming at the interface between the electrode and the polymer. Although a complete understanding of fundamental actuation mechanisms in ionic polymer transducers is still under debate, it is generally accepted that ion accumulation near the polymer-metal interface strongly correlates with generated strain.

Theoretical models providing a direct comparison between experiment and theory can be generally separated into phenomenological models based on curve fits of experimental data [10,11,12,13] and physical models that attempt to predict the material response from governing equations [7,14,15,16].

In this work a chemo-electrical model developed earlier by Wallmersperger [14,15] is experimentally calibrated. The chemo-electrical model is based on the one-dimensional Nernst-Planck equations for charge conduction considering the effects of charge gradients and electric potential gradients in space and time. This model allows us to compute the charge density as a function of applied electric field and electro-chemical boundary conditions in ionic polymer transducers. This study will therefore provide a direct comparison between experimental results and theory of actuation in ionic polymers.

In the first section the governing equations and the modeling approach are

given. The second section presents the numerical simulations and provides a parametric study of the physical parameters and the electro-chemical response of the ionomer. This study is aimed at providing a fetch table for model calibration performed in section three. Section four presents the experimental setup and procedures. The last section shows a comparison between numerical simulations and experimental results.

2 MODELING

In this section the chemo-electrical model is described and the formulation is presented. The following multi-field model describes the chemo-electrical behavior inside an ionic polymer transducer [14,15]. The formulation is capable of computing the ion distribution and the electric potential in the material as a function of space and time.

2.1 Chemical Field

The formulation for the chemical field is based on the balance equation for the flux of the mobile ions and fixed charges. Using the conservation of mass and the (one-dimensional) Nernst-Planck equation for the flux, the convection-diffusion equation for each species α

$$\dot{c}_\alpha(x,t) = \Big[D_\alpha\, c_{\alpha,i}(x,t) + z_\alpha\, c_\alpha(x,t)\, \mu_\alpha\, \Psi_{,i}(x,t)\Big]_{,i} \tag{1}$$

is obtained. The variable c_α is the concentration of the species α, D_α the diffusion constant, $\mu_\alpha = \frac{F}{RT}\, D_\alpha$ is the unsigned mobility, z_α is the valence of the ions, and Ψ is the electric potential. The notation ${}_{,i} = \frac{\partial}{\partial x_i}$ denotes the partial derivative with respect to x_i.

2.2 Electrical Field

The electric field is described by the quasi static Poisson equation

$$\Psi_{,ii}(x,t) = -\frac{F}{\varepsilon\,\varepsilon_0}\sum_{\alpha=1}^{N_f+N_b}\left(z_\alpha\, c_\alpha(x,t)\right)\,. \tag{2}$$

where ε_0 is the permittivity of free space, ε is the relative dielectric constant, N_A is the Avogadro constant, e is the electric elementary charge and F is the Faraday constant ($F = N_A \cdot e = 96487\,\mathrm{C/mol}$). N_f and N_b denote the number of freely movable species and the number of bound species, respectively.

2.3 Boundary Conditions at the Electrodes

In order to solve the given equations, boundary conditions for both the chemical and electrical field have to be specified. For the electric field, we prescribe the electric potential at both domain (electrode) boundaries. For the chemical field, a zero-flux $J_{\alpha\,i}(x_i,t)$ over the polymer-electrode boundary

$$-\,D_\alpha\, c_{\alpha,i}(x,t) - \frac{F}{RT}\,z_\alpha\, D_\alpha\, c_\alpha(x,t)\,\Psi_{,i}(x,t) \;= 0 \tag{3}$$

is prescribed.

2.4 Current Density and Charge Density

The ion transport in the polymer is directly related to the charge density (distribution)

$$\rho(x,t) = F\sum_{\alpha=1}^{N_f+N_b}\left(z_\alpha\, c_\alpha(x,t)\right). \tag{4}$$

The surface charge per unit area, $q^s(t)$, induced by the existence of a non-zero charge density $\rho(x,t)$ within the sample is obtained by an integration in the x-(thickness) direction

$$q^s(t) = \frac{1}{2h} \int_{-h}^{h} x\rho(x,t)dx. \tag{5}$$

The resulting current per unit area $i(t)$ is the time derivative of the induced surface charge,

$$i(t) = \frac{dq^s(t)}{dt}. \tag{6}$$

The surface charge and current are computed by Eqs. (5) and (6), respectively, using the discretized solution of the transport analysis.

3 NUMERICAL SIMULATION

Trends in the current density and the charge density are presented in this section as a function of the dielectric permittivity ϵ_r and the diffusion constant D. These trends will be used later to calibrate the model with the experimental results, and could be used in any future model calibration.

In the presented model, an ionic polymer transducer strip with thickness $2h = 200\mu m$, see Fig. 1, is considered.

The parameters for the numerical simulation are given in Tab. 1.

Trends between current and charge densities as a function of the permittivity and diffusion are obtained first. In Fig. 2, the current density i and the charge density q are plotted versus time for the permittivity values of $\epsilon_r = 40$, 60, and

80. The values for the diffusion constant $D = 2 \cdot 10^{-11}\, m^2/s$ and the applied voltage $U = 0.2V$ are held constant. The reference (solid) line represents the current response for $\epsilon_r = 40$, while the other two curves represent the simulated response for $\epsilon_r = 80$ and $\epsilon_r = 20$, respectively. As can be seen, the peak current density, i.e. $\widehat{i} = i(t \to 0+)$ is independent of the permittivity ϵ_r at constant D, while the rate of decrease of the peak is faster for smaller ϵ_r. This results in a larger decay time for a smaller value of ϵ_r. For this reason, the charge density, which is the integral of the current density, increases for increasing ϵ_r. This result is also shown in Fig. 2 (left). The tangent to the curve of the charge density at $t = 0$ remains constant for different permittivities, this is due to the same peak current density.

In Fig. 3, the current density i and the charge density q versus time for different diffusion constants are computed; in these numerical simulations the permittivity $\epsilon_r = 40$ and the applied voltage $U = 0.2V$ are held constant. The peak current density observed in Fig. 3, increases with a larger diffusion constant. On the other hand, the time decreases for a larger diffusion constant. This means that the ions move faster due to the higher D, but the total flux, the integral of the current density remains the same. This phenomenon can be seen in Fig. 3 (right): The final charge density ($q_{max} = q(t \to \infty)$) remains the same, independent of the diffusion constant.

Trends provided in both, the charge density and the current density plots, demonstrate the capability of the model to be calibrated with the experimentally obtained results. The diffusion constant and permittivity in the model will be used as the calibration variables.

Note that the qualitative behavior of the peak current density and the charge density as a function of the diffusion constant and the permittivity are given

in Tab. 2.

Tab. 2 presents a combination of results for different values of the dielectric constant and diffusion constant. It has been observed that the peak current density $\widehat{i}$ is proportional to the diffusion constant D but is not dependent on the permittivity ϵ_r. The maximal charge density is proportional to the square root of the permittivity, i.e. $q_{max} \sim \sqrt{\epsilon_r}$, but independent of the diffusion constant.

In Fig. 4 the current density and charge density versus time are plotted for different applied voltages at constant D and constant ϵ_r. As it can be noticed, the peak current density scales linearly with the applied electric voltage, while the charge density scales in a nonlinear fashion. Therefore, for larger applied electric potentials, the increase of the charge density becomes smaller. This is also demonstrated later in Fig. 7, where the steady state charge density is shown.

4 EXPERIMENTAL METHODS

The numerical model presented in the previous section is validated using experimental data. For this purpose an experimental setup was built and Nafion samples were tested. As mentioned in the introduction, an ionic polymer transducer consists of an ionomer membrane sandwiched between two layers of high surface area electrodes. The high surface area electrode is made of a mixture of electrically conductive particles uniformly distributed in an ionomer matrix. This configuration is complicated to model and hence flat plate electrodes are replaced in the simulations. In the experimental setup flat plates of gold, silver and copper with an area of 2 $cm \times 2$ cm were prepared. The flat plates tightly

sandwich a 200 micron thick Nafion sample. The area of the water-hydrated Nafion sample is approximately 2.4 $cm \times 2.4$ cm.

4.1 Sample Preparation

The ionomer samples are cut from a sheet of Nafion 117 sample purchased from FuelCell.com. Each sample is boiled in 1M Sulfuric acid for one hour and later boiled in de-ionized water for another hour. All the beakers and containers used in this study are thoroughly cleaned with de-ionised water. The de-ionised water source is a "Barnstead ultra pure water" that provides a water with 18.2 $\Omega\, cm$.

4.2 Current Measuring Experimental Setup

An electric circuit is built in order to measure the current flowing into the ionomer sample which is in contact with two flat electrodes. The schematics of the circuit are shown in Fig. 5. A potential step input is generated using a National Instruments DaqCard 6062E board. The power of the generated step signal is amplified using an HP current amplifier. The output voltage of the current sensing circuit is measured along with the voltage across the ionomer sample also using the NI 6062E DAQ board. The analog input sampling frequency is set to 200kHz. The experiment is repeated five times for a 0.1V, 0.2V, 0.5V, 1V, and a 2V applied step potential. The low applied potential is chosen to obtain current data with only ion transport in the membrane, while the high potential induces redox chemical reactions where an ion flux through the electrodes takes place. In all experiments the sample and the metal electrodes are submerged in de-ionised water. The current density $i(t)$ is computed

according to

$$i(t) = \frac{i_m(t)}{A}, \tag{7}$$

where $i_m(t)$ is the measured current, and A is the area of the electrodes. The charge density $q(t)$ is computed according to

$$q(t) = \int_0^t (i(\tau) - i_{ss}) d\tau, \tag{8}$$

where i_{ss} is the steady state value of the current density. The steady state value, is subtracted from the original current density to account for ion transport with blocking electrodes. In the numerical model the flux of ions through the electrodes, which is assumed to be due to the redox reactions, is not modeled. Finally the time decay is computed as the time at which 33% of the peak value is reached. Experiments are performed and presented in the next section. A comparison with the numerical simulations is also performed.

5 EXPERIMENTAL RESULTS AND DISCUSSION

In this section the experimental investigations are performed and compared to the numerical model. A proton based 2.4 $cm \times 2.4$ cm Nafion 117 sample was prepared according to the procedures detailed in the previous section. The ionomer sample was tested for 0.1V, 0.2V, 0.4V, and 1V when sandwiched with gold, silver, and copper electrodes, during separate experiments.

Presented in Fig. 6 (left) is the measured current density normalized according to Eq. (7) for the applied electric potentials $U = 0.1V, 0.2V, 0.5V, 1V$ on copper electrodes. This figure clearly demonstrates that the peak value of the current increases proportional to the applied potential. The peak current varies from

6.4 mA/cm^2 for a 0.1V potential to 80 mA/cm^2 for a 1V potential. The steady state current remains approximately zero for all applied potentials. The charge density which is computed according to Eq. (8) increases for a higher applied potential.

The charge density reaches the maximum value approximately 0.05 sec after the step is applied. Values of the steady state charge density increase from 5 $\mu C/cm^2$ for a 0.1V applied potential up to 54 $\mu C/cm^2$ at 1V. The numerical model is calibrated by the experimentally measured peak current density and steady state charge density for the copper flat electrode. This calibration is performed by determining the dielectric permittivity and the diffusion constant as explained in section 3. The values used for the numerical simulations are provided in Tab. 3.

Shown in Fig. 7 (left) is a comparison between the experimentally measured and numerically computed peak current density. The sample used in this experiment is a Nafion 117 membrane sandwiched between two flat copper electrodes. The calibration is performed at 0.1V and hence numerical and experimental values match. The values at 0.2V and 0.5V are nearly identical, while the experimental peak current density is approximately 18% larger than the numerical value. The steady state charge density comparison is shown in Fig. 7 (right). The prediction of our chemo-electrical model is very promising. The maximum difference is around 10%, and most important the numerical simulations and the experimental simulations follow a similar curve shape. The difference in the values could be explained by the fact that redox reactions occuring at the electrodes are not captured by the model. This could also explain the large peak current density at 1V.

Most physics-based models ([17,9]) increase the dielectric permittivity and the

value of the diffusion constant in order to match the experimental data of an ionic polymer transducer. Shown in Fig. 8 is the current density (left) and the charge density (right) of two proton Nafion 117 membranes under a 1V applied potential. The first sample is sandwiched between two flat gold electrodes while the second one has high surface area gold electrodes fabricated according to Oguro et al. [18]. The value of the peak current density has increased from 50 mA/cm^2 to 520 mA/cm^2. The decay time is computed to remain approximately the same for both samples at 1.2ms. Therefore, according to the theoretical trends presented earlier in Figs. 2 and 3, the diffusion constant is increased in order to model the effect of the high surface area electrode. Increasing the diffusion constant will decrease the decay time of the current density, and hence the dielectric permittivity has to be increased to match the decay time. On the other hand, observing the measured charge density in Fig. 8 (right) indicates that 10 times more ions are accumulated at the electrode. Increasing the dielectric permittivity will theoretically compensate this effect as shown in Fig. 2 (right).

In order to demonstrate this phenomenon, two numerical simulations, one with a dielectric permittivity of $\epsilon_r = 40$ and the other with $\epsilon_r = 400000$, have been performed. The simulated applied electric potential is 0.2V. The steady state normalized spacial charge across the thickness of the membrane is computed. Figure 9 (left) shows the charge accumulation near the cathode, and (right) the charge depletion region next to the anode. It could be noticed that more charges have accumulated next to the cathode while more charges depleted the anode for a higher dielectric permittivity.

The experimental comparison in charge accumulation for a flat electrode and a high surface area electrode is an interesting result which confirms previous

experimental results [6,19]. This result indicates the need for high surface area electrodes in ionic polymer transducers. This also supports the hypothesis that actuation mechanisms in ionic polymer transducers are due to the ion motion and accumulation on the electrode.

In the last set of experiments, the redox reactions between the electrode and the ionomer are studied. A proton based Nafion 117 ionomer is sandwiched between copper, silver, and gold electrodes and current and charge density data are obtained according to the procedures explained earlier. The experiment is run at 0.2V and 1V and the current density is shown in Fig. 10 (left) and (right), respectively. It could be noticed that at a low potential of approximately 0.2V, there are no redox reactions and the steady state current goes to zero for all samples. At a potential level of 1V (Fig. 10 (right)) the steady state current increases proportional to the electrochemical stability of the metal at the electrode. Copper shows the most redox reactions, followed by silver, while gold also shows a nearly zero steady state current. Previously in literature the steady state current has been correlated with the back relaxation in ionic polymer transducers [20].

6 CONCLUSION

In this study we have calibrated a numerical chemo-electrical model which is based on the Nernst-Planck equations for charge conduction in an ionic polymer transducer. Initially, trends between the dielectric permittivity and the diffusion constant with the electric response are presented. Increasing the permittivity will result in a slower time decay at a constant peak current density for an applied electric potential step. The charge density accumulated

at the electrode also increases with the dielectric permittivity. Increasing the diffusion coefficient increases the peak current and results in a smaller time decay constant. The steady charge density remains constant independently of the diffusion. Experimental results are obtained for a proton based Nafion 117 sample sandwiched between gold, silver, and copper flat electrodes. A comparison between the experimental results and the numerical simulations for flat electrodes are in good agreement for both the peak current density and the charge density. The model is capable to predict the shape of the curve of the charge density as a function of the applied potential. Impregnating a high surface area gold electrode in the Nafion sample increases the peak current from 50 mA/cm^2 to 520 mA/cm^2 while the steady state charge density is increased by one order of magnitude approximately. In numerical simulations these trends are accounted for by increasing both permittivity and diffusion constants. Finally the steady state current is correlated with the chemo-electric stability of the metal in the electrode. Copper electrodes demonstrate the largest steady state current followed by silver while the current tends to zero for gold electrodes.

The fact that a high surface area electrode exists in an ionic polymer transducer explains the need for simulating higher values of dielectric and diffusion constants to match the experimental data.

References

[1] B. J. Akle, Characterization and modeling of the ionomer-conductor interface in ionic polymer transducers, Ph.D. thesis, Virginia Tech, etd-08162005-140651 (2005).

[2] M. Shahinpoor, Y. Bar-Cohen, J. Simpson, J. Smith, Ionic polymer-metal

composites (IPMCs) as biomimetic sensors, actuators and artificial muscles - a review, Smart Materials and Structures 7 (6) (1998) R15–R30.

[3] Y. Bar-Cohen (Ed.), Electroactive Polymer Actuators as Artificial Muscles, 2nd Edition, SPIE Press, Bellingham, WA, 2004.

[4] M. D. Bennett, D. J. Leo, Ionic liquids as solvents for ionic polymer transducers, Sensors and Actuators A: Physical 115 (2004) 79–90.

[5] M. Shahinpoor, K. Kim, Solid-state soft actuator exhibiting large electromechanical effect, Applied Physics Letters 80 (18) (2002) 3445–3447.

[6] B. J. Akle, M. A. Hickner, D. J. Leo, J. E. McGrath, Correlation of capacitance and actuation in ionomeric polymer transducers, Journal of Material Science 40 (2005) 3715–3724.

[7] S. Nemat-Nasser, Micromechanics of actuation of ionic polymer-metal composites, Journal of Applied Physics 92 (5) (2002) 2899–2915.

[8] D. J. Leo, T. Wallmersperger, K. Farinholt, Computational model of ionic transport and electromechanical transduction in ionomeric polymer transducers, in: Proceedings of the SPIE, Vol. Paper Number 5759-24, 2005.

[9] T. Wallmersperger, D. Leo, C. Kothera, B. Kröplin, Ionic polymer metal transducers under time-harmonic excitation - theory and experiment, in: 16th International Conference on Adaptive Structures and Technologies, 2005.

[10] R. Kanno, S. Tadokoro, T. Takamori, M. Hattori, Linear approximate dynamic model of icpf actuator, in: Proceedings of the IEEE International Conference on Robotics and Automation, 1996, pp. 219–225.

[11] K. M. Newbury, D. J. Leo, Linear electromechanical model of ionic polymer transducers part I: Model development, Journal of Intelligent Material Systems and Structures 14 (6) (2003) 333–342.

[12] K. M. Newbury, D. J. Leo, Linear electromechanical model of ionic polymer transducers part II: Experimental validation, Journal of Intelligent Material Systems and Structures 14 (6) (2003) 343–358.

[13] S. Nemat-Nasser, S. Zamani, Y. Tor, Effect of solvents on the chemical and physical properties of ionic polymer-metal composites, Journal of Applied Physics 99 (104902).

[14] T. Wallmersperger, B. Kröplin, Rainer, R. W. Gülch, Coupled chemo-electro-mechanical formulation for ionic polymer gels - numerical and experimental investigations, Mechanics of Materials 36 (5-6) (2004) 411–420.

[15] T. Wallmersperger, B. Kröplin, R. W. Gülch, Electroactive Polymer (EAP) Actuators as Artificial Muscles - Reality, Potential, and Challenges; Second Edition, Vol. PM 136, SPIE Press, Bellingham, WA, USA, 2004, Ch. Modelling and Analysis of Chemistry and Electromechanics, pp. 335–362.

[16] X. Wang, B. Shapiro, E. Smela, Modeling charge transport in conjugated polymers, in: Y. Bar-Cohen (Ed.), Proceedings of the SPIE: Smart Structures and Materials 2006: Electroactive Polymer Actuators and Devices (EAPAD), Vol. 6168, SPIE, 2006.

[17] K. Farinholt, Modeling and characterization of ionic polymer transducers for sensing and actuation, Ph.D. thesis, Virginia Tech, etd-11232005-123339 (2005).

[18] K. Oguro, N. Fujiwara, K. Asaka, K. Onishi, S. Sewa, Polymer electrolyte actuator with gold electrodes, in: Proceedings of the SPIE, Vol. 3669, 1999, pp. 63–71.

[19] N. Fujiwara, K. Asaka, Y. Nishimura, K. Oguro, E. Torikai, Preparation of gold-solid polymer electrolyte composites as electric stimuli-responsive materials, Chem. Mater. 12 (6) (2000) 1750–1754.

[20] W. Robinson, Charge control of ionic polymers, Master's thesis, Virginia Tech, etd-08022005-095016 (2005).

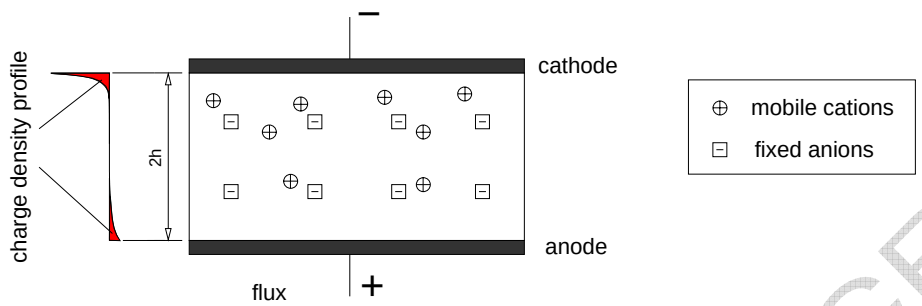

Fig. 1. IPMC strip

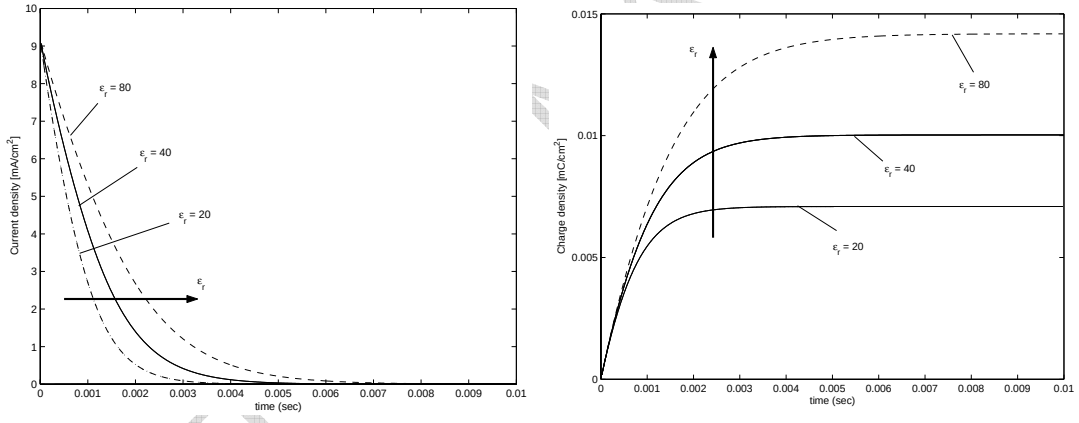

Fig. 2. Current density i (left) and charge density q (right) for $D = 2 \cdot 10^{-11} m^2/s$ and $\epsilon_r = 20; 40; 80$

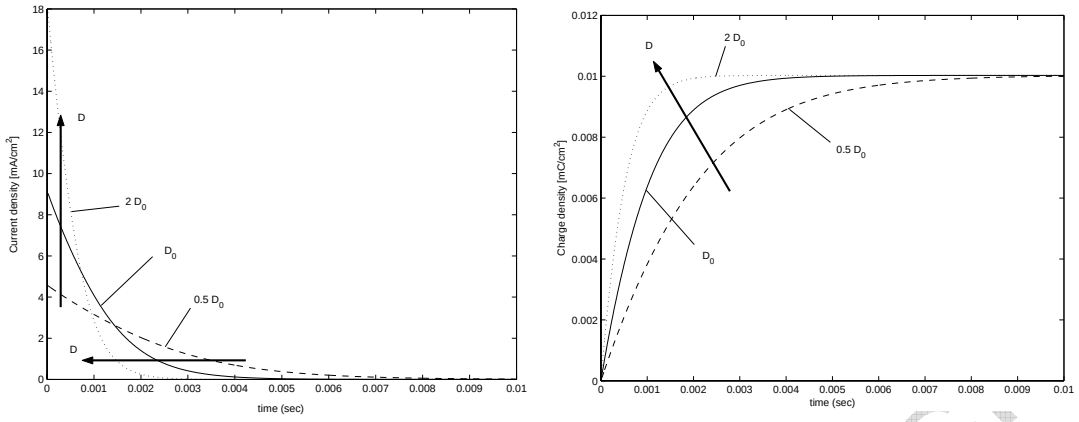

Fig. 3. Current density i (left) and charge density q (right) for $D = 0.5D_0; D_0, 2D_0$ (where $D_0 = 2 \cdot 10^{-11} m^2/s$) and $\epsilon_r = 40$

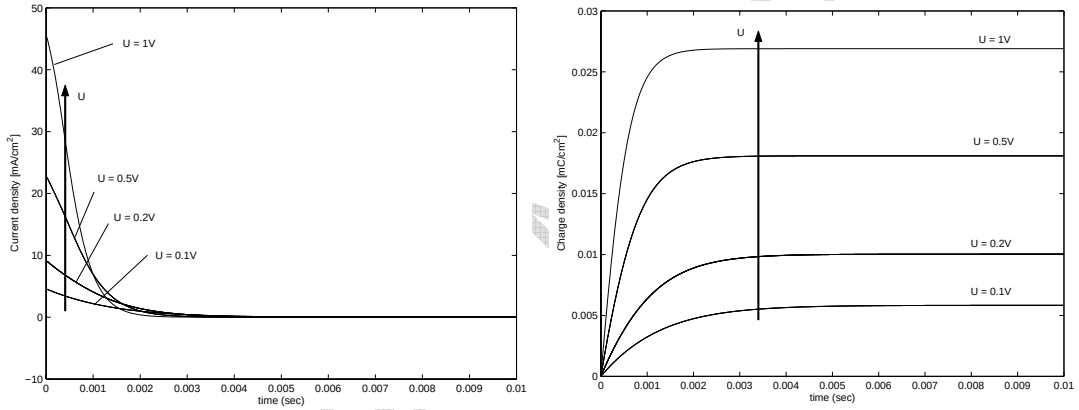

Fig. 4. Current density i (left) and charge density q (right) for $D = 2 \cdot 10^{-11} m^2/s$ and $\epsilon_r = 40$ for different applied electric potentials $U = 0.1V; 0.2V; 0.5V; 1V$

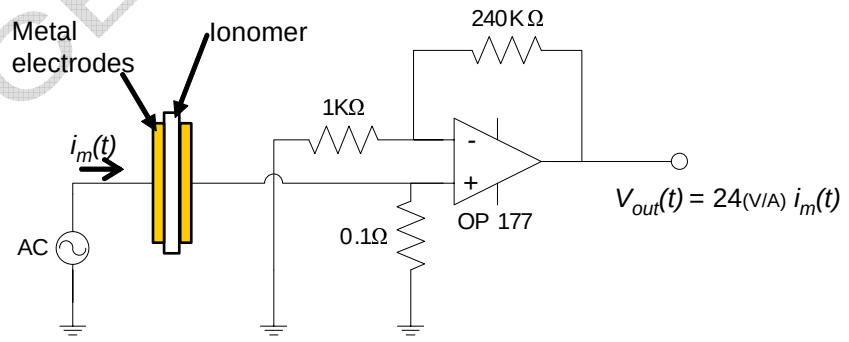

Fig. 5. Schematic of the experimental setup used to measure current flowing in the ionomer membrane.

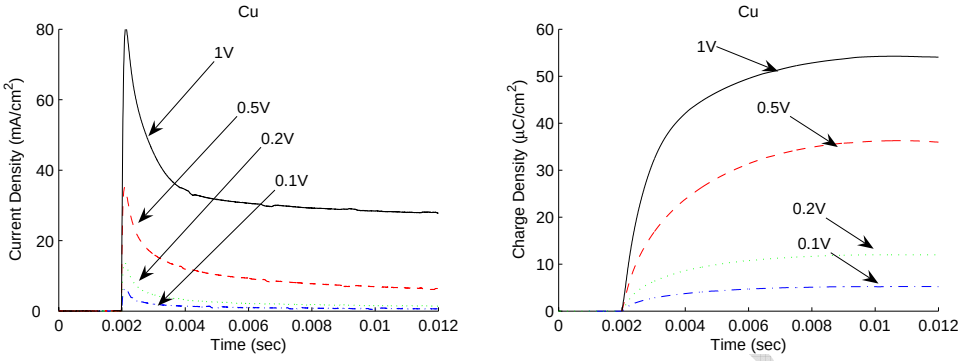

Fig. 6. Measured current density i (left) and charge density q (right) for the applied electric potentials $U = 0.1V; 0.2V; 0.5V; 1V$ using copper electrodes

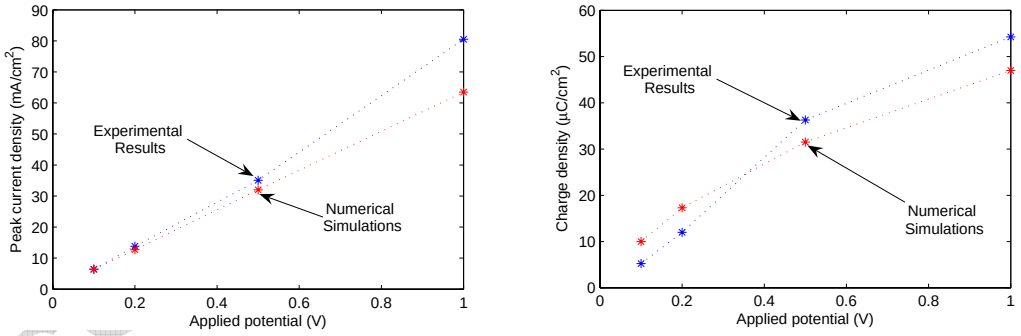

Fig. 7. A comparison between experimental and numerical peak current density i (left) and steady state charge density q (right) for the different applied electric potentials $U = 0.1V; 0.2V; 0.5V; 1V$ on copper electrodes

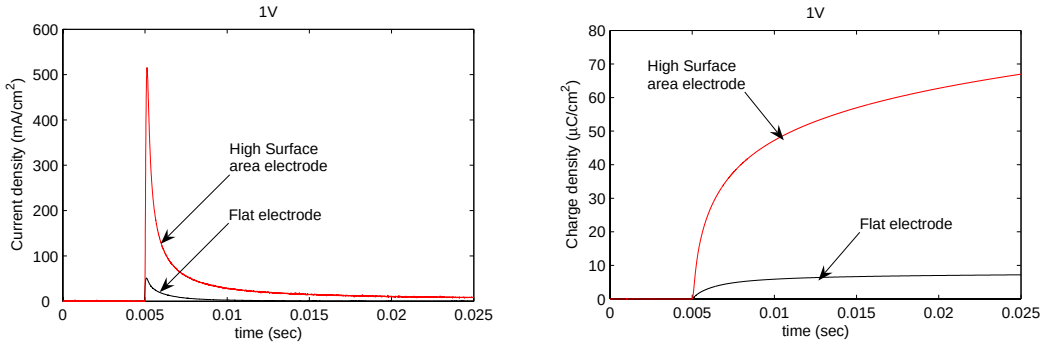

Fig. 8. Measured current density i (left) and charge density q (right) for an applied electric potential $U = 1V$ using flat and high surface area gold electrodes

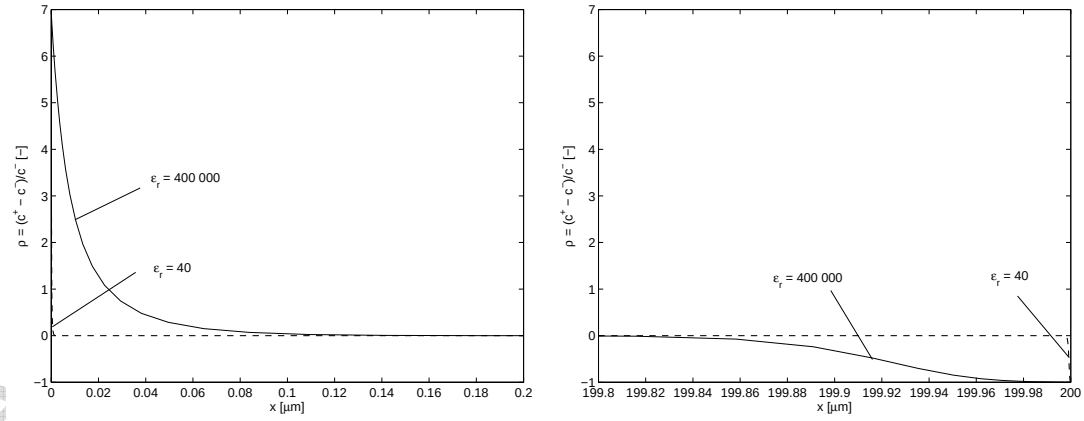

Fig. 9. Normalized charge density $\widetilde{\rho} = \frac{c^+ - c^-}{c^-}$ in steady-state versus x at the cathode side (left) and at the anode side (right) for two different permittivities.

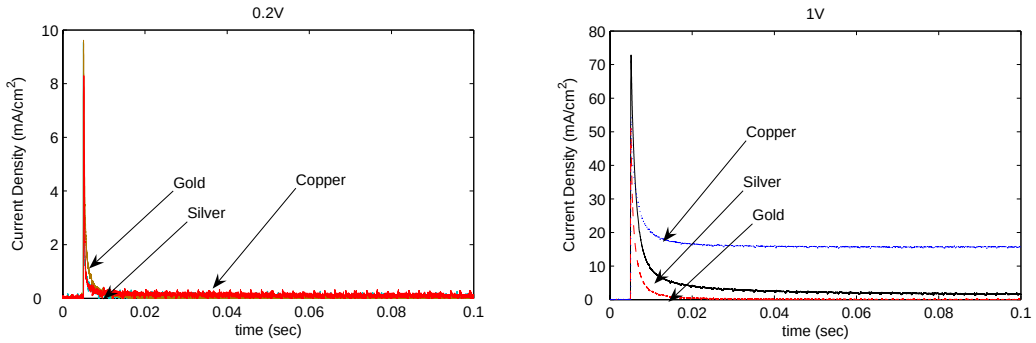

Fig. 10. Current density i for gold, silver and copper flat electrodes under a 0.2V applied potential (left) and 1V applied potential (right)

Table 1

Simulation parameters

Parameter	Variable	Value
Polymer thickness	$2h$	$200\,\mu m$
Anion concentration	c^-_{fix}	$1200\,mol/m^3$
Temperature	T	$293\,K$

	$\epsilon_r = 20$	$\epsilon_r = 40$	$\epsilon_r = 80$	$\epsilon_r = 4 \cdot 10^3$
$D = 1 \cdot 10^{-11}\ \frac{m^2}{s}$		$\widehat{i} = 4.6\ \frac{mA}{cm^2}$ $q_{max} = 10.1\ \frac{\mu C}{cm^2}$	$\widehat{i} = 4.6\ \frac{mA}{cm^2}$ $q_{max} = 14.2\ \frac{\mu C}{cm^2}$	$\widehat{i} = 4.6\ \frac{mA}{cm^2}$ $q_{max} = 101\ \frac{\mu C}{cm^2}$
$D = 2 \cdot 10^{-11}\ \frac{m^2}{s}$	$\widehat{i} = 9.1\ \frac{mA}{cm^2}$ $q_{max} = 7.1\ \frac{\mu C}{cm^2}$	$\widehat{i} = 9.17\ \frac{mA}{cm^2}$ $q_{max} = 10.1\ \frac{\mu C}{cm^2}$	$\widehat{i} = 9.17\ \frac{mA}{cm^2}$ $q_{max} = 14.2\ \frac{\mu C}{cm^2}$	$\widehat{i} = 9.17\ \frac{mA}{cm^2}$ $q_{max} = 101\ \frac{\mu C}{cm^2}$
$D = 1 \cdot 10^{-10}\ \frac{m^2}{s}$		$\widehat{i} = 45.9\ \frac{mA}{cm^2}$ $q_{max} = 10.1\ \frac{\mu C}{cm^2}$		$\widehat{i} = 45.9\ \frac{mA}{cm^2}$ $q_{max} = 101\ \frac{\mu C}{cm^2}$

Table 2

Resulting peak current density $\widehat{i}$ and maximal charge density q_{max} for different permittivities ϵ_r and diffusion constants D at an applied voltage $U = 0.2V$

Table 3

Simulation parameters: dielectric permittivity and diffusion constant

Parameter	Variable	Value
Dielectric permittivity	ϵ_r	120
Diffusion coefficient	D	$2.8 \cdot 10^{-11} m^2/s$